Lithium Ion Batteries

DOI: 10.1002/ange.201305375

Experimental Confirmation of Low Surface Energy in $LiCoO_2$ and Implications for Lithium Battery Electrodes**

*Pardha S. Maram, Gustavo C. C. Costa, and Alexandra Navrotsky**

Diversifying the applications of lithium ion batteries (LIBs) demands the development of better cathode materials with faster ionic diffusion, as well as improved fundamental understanding of what factors enhance or compromise performance. It has been proposed that reducing the dimensions of cathode materials to the nanoscale enhances the kinetics of Li-ion diffusion, resulting in high charge/discharge rate capabilities.[1–4] However, deleterious "nano effects" due to altered surface structure (atomic arrangement, transition metal oxidation state, and electronic structure) may strongly affect the surface energetics which in turn significantly alter the cell voltage and reversibility.[5,6] Knowing the surface structure, bonding, and thermodynamics of nanoscale oxides is essential for rational tuning of their performance as electrode materials, both in terms of safe operation and enhanced electrochemical behavior.

Recently, dramatic thermodynamic shifts in the position of oxidation–reduction equilibria for various nanoscale transition metal oxide systems (Co–O, Fe–O, Mn–O) have been reported.[7,8] When the particle size is reduced to a few nanometers, the surface-to-volume ratio enormously increases, and surface energy can contribute significantly to the total free energy. Thus, differences in surface energy may affect the thermodynamic driving force for various processes, including the phase transition from layered rocksalt to spinel in $LiCoO_2$, oxidation–reduction (the cell voltage itself may be affected), and the binding of molecules and ions, including H_2O and Li^+, to the surface.

Since surfaces of nanoscale materials are reactive, water adsorption is almost unavoidable.[9–11] It has been shown for $Li[Li_{1/3-2x/3}Ni_xMn_{2/3-x/3}]O_2$ that the reversible discharge capacity is affected by surface adsorbed hydroxy groups (-OH).[12] For the same structural family, even degassing under ultra-high vacuum at 350 °C is not sufficient to eliminate the hydroxy groups, which remain on about one third of the surface monolayer.[9] Such surface adsorbed water may be detrimental to battery performance since it can induce electrolyte decomposition and increase polarization.[13]

Additionally, Okubo et al. showed that extreme size reduction of $LiCoO_2$ below 15 nm does not yield good reversibility toward Li (de)intercalation.[6] They suggested that these effects might be due to the presence of Co^{2+} ions near the surface, giving stoichiometry $Li_{1+x}Co_{2+x}Co_{3+1-x}O_2$. According to Levasseur et al.,[14] oxygen vacancies are present near the surface, but Co^{2+} ions are not. This leads some Co^{3+} to assume square-based pyramidal coordination with an intermediate spin configuration. Recently, Qian et al.[15] obtained experimental evidence of an electronic spin transition in nanophase stoichiometric $LiCoO_2$. They also showed that surface energies computed using density functional theory (DFT) were quite low (about 1.2 $J\,m^{-2}$), and decreased further when the Co^{3+} electronic spin state near the surface changed from low-spin (LS) to high-spin (HS) or intermediate-spin (IS) states. The predicted surface energies currently lack experimental validation.

In light of surface electronic spin transition effects and surface adsorbed water in $LiCoO_2$, we show here, by direct oxide melt solution calorimetric measurements, that the surface energy of ordered rocksalt lithium cobalt oxide, $LiCoO_2$, one of the most studied materials for battery applications, is substantially lower than that of simple rocksalt oxides CoO and NiO. The measured enthalpy of water adsorption to the surface of nanoscale $LiCoO_2$ is found to be significantly less exothermic than on CoO, NiO and other binary transition metal oxides. The labile surface water may aid in transfer of lithium ions across the electrolyte–electrode interface. These observations suggest that strategies for further developing LIB electrodes should focus on the search for materials with low surface energies.

Stoichiometric $LiCoO_2$ samples with extremely small crystallite sizes were prepared by a hydrothermal intercalation method following Okubo et al.[5,6] Commercial $LiCoO_2$ was used as a reference to bulk. The commercial sample was annealed at 900 °C for 6 h to eliminate any possible low-temperature $LiCoO_2$ phase. Chemical analysis was carried out using inductively coupled plasma optical emission spectroscopy (ICP-OES). The compositions of all nanoscale $LiCoO_2$ samples are stoichiometric within the experimental error (Table 1). Powder X-ray diffractograms for all samples confirm formation of single-phase $LiCoO_2$ (Supporting Information, Figure S1). The observed background is due to the fluorescence of cobalt under $Cu_{K\alpha}$ radiation. The crystallite size calculated from powder X-ray diffraction varies from 9.4 ± 0.4 to 29.1 ± 1.1 nm, similar to that of Okubo et al.[5,6] For the end members (sample 1 and bulk), synchrotron X-ray diffraction data were collected (ALS 11-BM via the mail-in

[*] P. S. Maram, G. C. C. Costa, A. Navrotsky
Peter A. Rock Thermochemistry Laboratory and NEAT ORU
University of California Davis
One Shields Avenue, Davis, CA (USA)
E-mail: anavrotsky@ucdavis.edu
Homepage: http://www.navrotsky.engr.ucdavis.edu

[**] This work was supported by the U.S. Department of Energy, grant DEFG02-03ER46053. We acknowledge ALS 11-BM (Advanced Light Source) for mail-in synchrotron diffraction service. We thank Josh D. Furman for preliminary experiments and Tien Tran for useful discussions.

Supporting information for this article is available on the WWW under http://dx.doi.org/10.1002/anie.201305375.

Table 1: Summary of data used for the calculation of corrected drop solution enthalpies of the $LiCoO_2$ nanoscale powders.

Sample	Crystallite size XRD [nm]	BET S.A. [$m^2\,mol^{-1}$]	Composition by ICP-OES [mol] Li	Co	H_2O [mol] adsorbed on $LiCoO_2$ surface Physically	Chemically	Corrected enthalpy ΔH_{ds} [$kJ\,mol^{-1}$] For hydrated surface	For anhydrous surface
1	9.4 ± 0.4	5510 ± 55	1.07 ± 0.02	0.99 ± 0.02	0.190 ± 0.013	0.056 ± 0.002	110.96 ± 2.05	110.04 ± 2.06
2	11.9 ± 0.1	5060 ± 55	1.02 ± 0.03	1.00 ± 0.02	0.141 ± 0.003	0.051 ± 0.002	111.71 ± 1.70	110.87 ± 1.70
3	19.9 ± 1.7	3834 ± 63	1.04 ± 0.03	1.02 ± 0.03	0.033 ± 0.03	0.039 ± 0.001	112.29 ± 0.58	111.65 ± 0.59
4	29.1 ± 1.1	1814 ± 26	1.01 ± 0.02	0.99 ± 0.03	0.033 ± 0.002	0.018 ± 0.001	114.67 ± 0.57	114.37 ± 0.57
bulk	>1000	46 ± 2	0.99 ± 0.02	1.00 ± 0.02	0	0	–	116.54 ± 0.45

service) and the structure ($R\bar{3}m$ space group) was refined using the Rietveld method. The observed, calculated, and difference patterns are shown in the Supporting Information (Figure S2). The obtained profile factors confirm good fitting quality. The synthesized nanophase stoichiometric $LiCoO_2$ exhibits very fine particles of plate-like morphology whose thickness increases from sample (1) to (4) as shown in Figure S3 (Supporting Information). Figure S3 (1) shows very fine particles of $LiCoO_2$ with hexagonal shape, and Figure S3 (4) clearly shows the layer stacking of $LiCoO_2$ particles.

$LiCoO_2$ crystallizes in two crystallographic modifications; low-temperature (LT) spinel (*Fd3m*) and high-temperature (HT) ordered layered rocksalt structure. The XRD patterns of the LT and HT phases are very similar, but show differences in relative intensities. However, the vibrational spectra show distinct differences. The irreducible representation for the vibrational modes of layered $LiCoO_2$ by factor group analysis is $A_{1g}+2A_{2u}+E_g+2E_u$.[16,17] The gerade modes are Raman active, and the ungerade modes are IR active. Therefore vibrational spectroscopy is more sensitive to the structural difference than XRD and the presence of a well-defined layered structure was confirmed by FTIR and Raman spectroscopy, as shown in Figure S3 and S4 (Supporting Information), with four bands for FTIR and two bands for Raman clearly identifying the layered structure.

The Brunauer–Emmett–Teller (BET) surface area of the $LiCoO_2$ nanoparticles decreases with increasing crystallite size (sample 1 to 4). The total water contents (n) for the samples introduced into the calorimeter were determined by thermogravimetric analyses on 10–20 mg pellets. The samples were heated to 600 °C in dry air at 5 °C min^{-1} and held for 3 h to complete dehydration. No further mass changes were observed upon heating to 850 °C.

The enthalpy of water chemisorption to the surface of $LiCoO_2$ nanoparticles was determined using microcalorimetry in conjunction with a water vapor dosing system (Section 3 in the Supporting Information).[18,19] Figure 1 compares the differential heats of water adsorption vs. coverage for $LiCoO_2$ and CoO. The first dose of water vapor gives a strongly exothermic heat of adsorption ($-158\,kJ\,mol^{-1}$ H_2O), which is nevertheless approximately 60% smaller in magnitude than that for rocksalt CoO ($-256\,kJ\,mol^{-1}$ H_2O).[7] The differential adsorption enthalpy becomes less exothermic as the water coverage increases. The total water coverage at the dose where the differential enthalpy of adsorption reaches $-44\,kJ\,mol^{-1}$ (the enthalpy of condensation of water vapor at room temperature) for $LiCoO_2$ (6.08 ± 0.2 $H_2O\,nm^{-2}$) is much smaller than for CoO (15.24 ± 0.4 $H_2O\,nm^{-2}$). The total integral enthalpy of water adsorption (ΔH_{ads}) for $LiCoO_2$ at that coverage ($-60.5\pm1.5\,kJ\,mol^{-1}$ H_2O) is less exothermic than for CoO ($-82.3\pm1.6\,kJ\,mol^{-1}$ H_2O).[7,20] Thus $LiCoO_2$, which is a LIB material, has lower surface energy and weaker water adsorption than CoO and NiO which are not suitable battery materials.

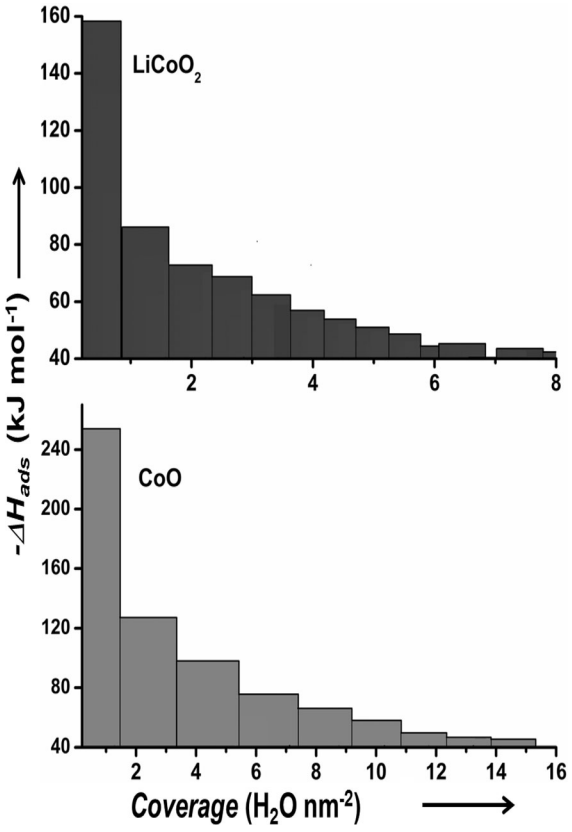

Figure 1. Measured differential heats of adsorption, ΔH_{ads} [$kJ\,mol^{-1}$] on the surface of nanophase CoO and $LiCoO_2$ as a function of surface coverage. The CoO water adsorption data are from Navrotsky et al.[7]

This pattern of lower water coverage and weaker water binding to the surface is also observed in our recent studies of nanophase tin dioxide and calcium manganese oxide. These two systems both show low affinity for water binding to the surface and low surface energy. Recently, Castro and Quach[21] documented a general relationship between water adsorption behavior and surface energy: the more exothermic the water adsorption enthalpy of a material, the greater its surface energy. The present data support this correlation.

Using calorimetric methods, we determined the drop solution enthalpy for $LiCoO_2$ samples of different surface areas. The drop solution enthalpies were corrected for physically and chemically adsorbed water to determine the enthalpies of the hydrous and anhydrous surfaces, respectively. The thermochemical cycles used for water correction and further information about the calculations are given in the Supporting Information (Section 3). A summary of chemical analysis, BET surface area, and water adsorption data used for the calculations is given in Table 1.

Figure 2 shows the water-corrected enthalpies of drop solution versus BET surface area for nanophase $LiCoO_2$.

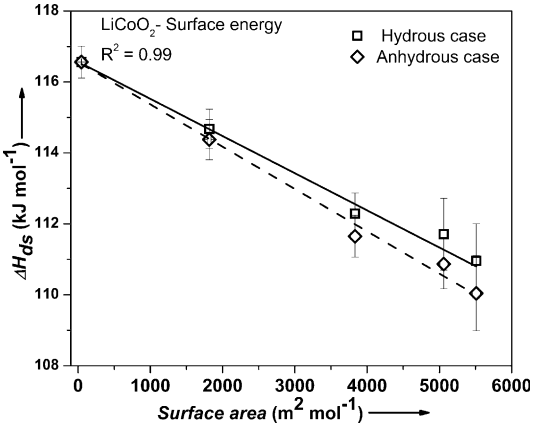

Figure 2. Drop solution enthalpies of nanophase $LiCoO_2$ vs. surface area, corrected for water content as described in the text.

Fitting a line to these two sets of corrected data, the slope gives the enthalpy of the hydrous and anhydrous surfaces, $1.11 \pm 0.05\ J\,m^{-2}$ and $1.25 \pm 0.05\ J\,m^{-2}$, respectively. The enthalpies for the hydrous and anhydrous surfaces are the same within experimental error, consistent with the finding that the integral enthalpy of water chemisorption ($\Delta H_{ads} = -60.5 \pm 1.5\ kJ\,mol^{-1}$) is only moderately more exothermic than the enthalpy of water condensation ($-44\ kJ\,mol^{-1}$). From these results, we conclude that water adsorption on $LiCoO_2$ does not play a major role in stabilizing the surface. The excess surface enthalpies of $LiCoO_2$, NiO and CoO nanoparticles relative to their bulk phases are given in Figure 3 to stress the difference in behavior between $LiCoO_2$ and the binary rocksalt oxides.

The experimental surface enthalpies are compared to previously reported DFT calculations of various low-index surfaces of $LiCoO_2$, and with the experimental results for other isostructural rocksalt oxides (Table 2). The surfaces of $LiCoO_2$ particles are terminated mainly by (001) planes, and that edges are dominated by the (104) and (110) planes.[22] According to Kramer et al.[22] and Qian et al.,[15] Co^{3+} on the (001) surface remains octahedrally coordinated with a LS configuration and does not have any unpaired electrons. However, on (104) and (110) non-polar surfaces, Co^{3+} ions are coordinated by five and four oxygen ions, respectively, resulting in a square pyramidal (IS) and pseudotetrahedral (HS) configuration, respectively. Thus, the missing Co–O

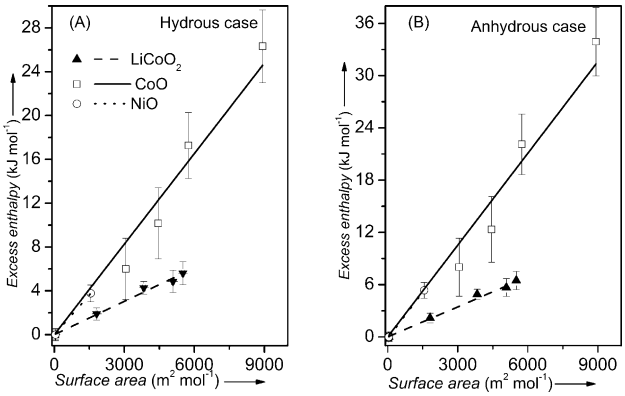

Figure 3. Enthalpy relative to bulk phase (excess enthalpy in $kJ\,mol^{-1}$, caused by increase in the surface area), plotted versus surface area for A) CoO, NiO and $LiCoO_2$ hydrous cases, B) CoO, NiO and $LiCoO_2$ anhydrous cases. CoO and NiO are reference values.

Table 2: Surface energy of $LiCoO_2$ and other rocksalt oxides comparison with previous theoretical studies.

Rocksalt phases	Calculated surface energy [$J\,m^{-2}$]	Experimental surface energy, [$J\,m^{-2}$]	
		Hydrous	Anhydrous
CoO	4.81[a]	2.82 ± 0.20	3.57 ± 0.30[c]
NiO	6.02[a]	2.40 ± 0.20	3.50 ± 0.50[c]
$LiCoO_2$	1.12 (LS); 0.312 (IS)[b] 1.23 (HS); 2.23 (LS)[b]	1.11 ± 0.05	1.25 ± 0.05

[a] Calculated data for oxygen-terminated relaxed (111) surface,.[23,24]
[b] Calculated data for (104) and (110) surfaces.[15] LS (low spin), IS (intermediate spin), and HS (high spin) electronic state of Co^{3+}.
[c] Experimentally measured data.[7]

bonds change the surface Co crystal field effects. As a result, the surface energies calculated from DFT are significantly reduced; i.e., from $1.12\ J\,m^{-2}$ (LS) to $0.32\ J\,m^{-2}$ (IS) for the (104) surface, and from $2.23\ J\,m^{-2}$ (LS) to $1.24\ J\,m^{-2}$ (HS) for the (110) surface, respectively. The measured surface energies are $1.11 \pm 0.05\ J\,m^{-2}$ (hydrous surface) and $1.25 \pm 0.05\ J\,m^{-2}$ (anhydrous surface). They agree well with those calculated by DFT. Although the majority of the $LiCoO_2$ surface is presumably composed of (001) planes, the experimental surface energy is an average of the contributions of a number of surface planes and defects on the actual particles. From Table 2, it is clear, from both theory and experiment, that $LiCoO_2$ has a lower surface energy than the simple rocksalt oxides CoO and NiO. Indeed the agreement between calorimetric and DFT values of surface energy of $LiCoO_2$, obtained completely independently, can be considered excellent benchmarking between both approaches.

This work suggests that the changes in coordination, valence, and spin state of cobalt near the surface of stoichiometric $LiCoO_2$, strongly affect the surface energy. The driving force behind the spin transition is change in the coordination geometry due to the oxygen loss at the surface. These changes near the surface have pros and cons for electrode function. They appear to deleteriously affect the voltage profile of lithium intercalation.[6,15] However, the low

surface energy and low water binding energy make the surface more reactive and more accessible for species from solution or the gas phase to active surface sites. Several nanostructured functional metal oxides ($LiCoO_2$ as an electrode material (this work), calcium manganese oxide as a water oxidation catalyst,[25] and tin oxide as a sensor[26]) show similarly low surface energies and water binding energies. The variability of surface oxidation states, local geometries, and spin states, as documented for $LiCoO_2$ and CaMnO may improve electron transfer (redox) in both a thermodynamic and kinetic sense. Work is underway to determine if this is indeed a general observation for redox active battery materials. We propose that, in seeking new electrode materials, one should consider low surface energy, which usually correlates with loosely bound surface water as a desirable attribute, which can potentially be screened for by DFT calculations on proposed new structures.

Experimental Section

CoOOH was prepared as a precursor to $LiCoO_2$ by oxidation of precipitated cobalt hydroxide.[27] For a typical preparation, 10 mmol of cobalt nitrate hexahydrate was dissolved into 50 mL millipore-filtered H_2O with mechanical stirring. This solution was poured slowly into 50 mL of 5 M NaOH, forming a pink-colored suspension. This suspension was diluted into 800 mL of H_2O and stirred for 48 h with air bubbling to promote oxidation. The suspended particles turned brown and were separated by centrifugation, washed three times with H_2O and ethanol to remove unreacted NaOH, and dried under vacuum at room temperature.

Nanocrystallites of $LiCoO_2$ were prepared by a hydrothermal intercalation method modified from that of Okubo et al.[5,6] For a typical reaction, 100 to 400 mg of the CoOOH precursor was thoroughly mixed with 15 mL of 1 M LiOH in a PTFE lined autoclave (Parr Instruments, 23 mL). These samples are referred to as Samples 1 (100 mg) to 4 (400 mg). The vessels were sealed and heated to 180 °C at 0.5 °C min^{-1} and held for 12 h. Products were separated by centrifugation, washed three times with water and ethanol, and dried at room temperature under vacuum.

Received: June 22, 2013
Revised: July 22, 2013
Published online: September 23, 2013

Keywords: layered compounds · $LiCoO_2$ · lithium ion batteries · surface energy · thermodynamics

[1] P. Poizot, S. Laruelle, S. Grugeon, L. Dupont, J. M. Tarascon, *Nature* **2000**, *407*, 496 – 499.
[2] H. Chen, C. P. Grey, *Adv. Mater.* **2008**, *20*, 2206 – 2210.
[3] F. Jiao, K. M. Shaju, P. G. Bruce, *Angew. Chem.* **2005**, *117*, 6708 – 6711; *Angew. Chem. Int. Ed.* **2005**, *44*, 6550 – 6553.
[4] M. G. Kim, J. Cho, *Adv. Funct. Mater.* **2009**, *19*, 1497 – 1514.
[5] M. Okubo, E. Hosono, J. Kim, M. Enomoto, N. Kojima, T. Kudo, H. Zhou, I. Honma, *J. Am. Chem. Soc.* **2007**, *129*, 7444 – 7452.
[6] M. Okubo, J. Kim, T. Kudo, H. Zhou, I. Honma, *J. Phys. Chem. C* **2009**, *113*, 15337 – 15342.
[7] A. Navrotsky, C. Ma, K. Lilova, N. Birkner, *Science* **2010**, *330*, 199 – 201.
[8] N. Birkner, A. Navrotsky, *Am. Mineral.* **2012**, *97*, 1291 – 1298.
[9] A. W. Moses, H. G. G. Flores, J.-G. Kim, M. A. Langell, *Appl. Surf. Sci.* **2007**, *253*, 4782 – 4791.
[10] A. Navrotsky, *ChemPhysChem* **2011**, *12*, 2207 – 2215.
[11] V. Alexandrov, T. Y. Shvareva, S. Hayun, M. Asta, A. Navrotsky, *J. Phys. Chem. Lett.* **2011**, *2*, 3130 – 3134.
[12] C. R. Fell, K. J. Carroll, M. Chi, Y. S. Meng, *J. Electrochem. Soc.* **2010**, *157*, A1202 – A1211.
[13] K. T. Lee, S. Jeong, J. Cho, *Acc. Chem. Res.* **2013**, *46*, 1161 – 1170.
[14] S. Levasseur, M. Menetrier, Y. Shao-Horn, L. Gautier, A. Audemer, G. Demazeau, A. Largeteau, C. Delmas, *Chem. Mater.* **2003**, *15*, 348 – 354.
[15] D. Qian, Y. Hinuma, H. Chen, L.-S. Du, K. J. Carroll, G. Ceder, C. P. Grey, Y. S. Meng, *J. Am. Chem. Soc.* **2012**, *134*, 6096 – 6099.
[16] H. Porthault, R. Baddour-Hadjean, C. Le, C. Bourbon, S. Franger, *Vib. Spectrosc.* **2012**, *62*, 152 – 158.
[17] S. Madhavi, R. Subba, B. V. R. Chowdari, S. F. Y. Li, *Electrochim. Acta* **2002**, *48*, 219 – 226.
[18] S. V. Ushakov, A. Navrotsky, *Appl. Phys. Lett.* **2005**, *87*, 164103.
[19] M. P. Saradhi, S. V. Ushakov, A. Navrotsky, *RSC Adv.* **2012**, *2*, 3328 – 3334.
[20] C. Ma, A. Navrotsky, *Chem. Mater.* **2012**, *24*, 2311 – 2315.
[21] R. H. R. Castro, D. V. Quach, *J. Phys. Chem. C* **2012**, *116*, 24726 – 24733.
[22] D. Kramer, G. Ceder, *Chem. Mater.* **2009**, *21*, 3799 – 3809.
[23] K. L. Yao, H. M. Huang, Z. L. Liu, *Phys. B Condens. Matter.* **2008**, *403*, 3191 – 3194.
[24] A. Wander, I. J. Bush, N. M. Harrison, *Phys. Rev. B* **2003**, *68*, 233405.
[25] N. Birkner, S. Nayeri, B. Pashaei, M. M. Najafpour, W. H. Casey, A. Navrotsky, *Proc. Natl. Acad. Sci. USA* **2013**, *110*, 8801 – 8806.
[26] Y. Ma, R. H. R. Castro, W. Zhou, A. Navrotsky, *J. Mater. Res.* **2011**, *26*, 848 – 853.
[27] V. Pralong, A. Delahaye-Vidal, B. Beaudoin, B. Gerand, J.-M. Tarascon, *J. Mater. Chem.* **1999**, *9*, 955 – 960.

